Published in final edited form as:
J Pain. 2009 July ; 10(7): 750–758. doi:10.1016/j.jpain.2009.01.264.

Sodium Channel Expression and Localization at Demyelinated Sites in Painful Human Dental Pulp

Michael A. Henry[*], **Songjiang Luo**[*], **Benjamin D. Foley**[†], **Rachael S. Rzasa**[†], **Lonnie R. Johnson**[†], and **S. Rock Levinson**[§]

[*]Department of Endodontics, University of Texas Health Science Center at San Antonio, San Antonio, Texas

[†]Department of Surgical Dentistry, University of Colorado Denver, Aurora, Colorado

[§]Department of Physiology and Biophysics, University of Colorado Denver, Aurora, Colorado

Abstract

The expression of sodium channels (NaCh(s)) change after inflammatory and nerve lesions and this change has been implicated in the generation of pain states. Here we examine NaCh expression within nerve fibers from normal and painful extracted human teeth with special emphasis on their localization within large accumulations, like those seen at nodes of Ranvier. Pulpal tissue sections from normal wisdom teeth and from teeth with large carious lesions associated with severe and spontaneous pain were double-stained with pan-specific NaCh antibody and caspr (paranodal protein used to visualize nodes of Ranvier) antibody, while additional sections were triple-stained with NaCh, caspr and myelin basic protein (MBP) antibodies. Z-series of images were obtained with the confocal microscope and evaluated with NIH ImageJ software to quantify the density and size of NaCh accumulations, and to characterize NaCh localization at caspr-identified typical and atypical nodal sites. Although the results showed variability in the overall density and size of NaCh accumulations in painful samples, a common finding included the remodeling of NaChs at atypical nodal sites. This remodeling of NaChs included prominent NaCh expression within nerve regions that showed a selective loss of MBP staining in a pattern consistent with a demyelinating process.

Keywords

dental pulp; demyelination; sodium channel; caspr/contactin; nodes of Ranvier; myelin basic protein

Author for Correspondence: Michael A. Henry, D.D.S., Ph.D., Department of Endodontics, Mail Code 7892, University of Texas Health Science Center at San Antonio, 7703 Floyd Curl Drive, San Antonio, TX 78229, Office telephone #: 210 567-0877, FAX telephone #: 210 567-3389, henrym2@uthscsa.edu.

Perspective

This study identifies the remodeling of NaChs at demyelinated sites within the painful human dental pulp and suggests that the contribution of NaChs to spontaneous pulpal pain generation may not only be dependant on total NaCh density but may also be related to NaCh expression at atypical nodal sites.

Introduction

The activation of voltage-gated sodium channel(s) (NaCh(s)) play an essential role in neuronal excitability, including the initiation and propagation of action potentials.[21] Experimental animal studies and fewer human studies have shown that NaChs change their expression in sensory neurons following inflammatory and nerve lesions, and these changes may contribute to the activation of pain pathways leading to the development of increased pain states.[4,11–12]

The dental pulp is a rich source of pain fibers and represents a valuable system to study peripheral pain mechanisms.[8] Additionally, there is an abundant supply of both extracted normal wisdom teeth and painful teeth with known pain levels that are available for study. We are using the human extracted tooth as a model system to evaluate human peripheral pain mechanisms and are applying quantitative methods that allow an objective comparison of NaCh expression in normal and painful samples. The purpose of this study was to quantify the density and size of significant NaCh accumulations within the pulpal nerve fibers from normal wisdom teeth and from carious molar teeth that were characterized by the presence of severe and spontaneous pain. Furthermore, we used an antibody against caspr (a paranodal protein) to characterize the expression of NaCh accumulations at typical and atypical nodal sites, and myelin basic protein (MBP) antibody to evaluate these expressions relative to state of myelination. The results of this study will further our understanding of how NaCh expressions are changed within painful human peripheral tissues and how these changes may contribute to the constant, increased evoked and spontaneous pain responses that characterize the pain associated with toothache. Part of this research was presented in Abstract form at an American Pain Society annual meeting.[28]

Materials and Methods

Human dental pulp collection and preparation

This study was approved by the University of Colorado Human Subjects Institutional Review Board and informed consent was obtained from each subject. Teeth were obtained from patients presenting to the University of Colorado School of Dental Medicine Clinics for the extraction of either a normal third molar (“wisdom” tooth that was erupted with fully developed apices) or a painful molar tooth diagnosed with irreversible pulpitis (n = 10 in each group; normal group included 7 males and 3 females with an average age of 24.4 +/−2.0 and with an age range of 18 to 36; painful group included 4 males and 6 females with an average age of 29.0 +/− 1.9 and with an age range of 20 to 42). The painful samples were limited to those with a large carious lesion that extended well into the pulpal tissues and that were associated with pain that was described as constant in character, that included the presence of sharp, shooting spontaneous pain episodes, and that was as rated as severe in intensity over the 24 hour time-period preceding the extraction. Additionally, all painful teeth showed transient or prolonged pain responses to cold, hot or electric pulp testing, thus demonstrating the presence of viable nerves. The extracted teeth were collected in 0.1 M phosphate buffer (PB) and a bur in a high-speed dental handpiece was used to place a groove around the tooth, while avoiding penetration into the pulpal tissues. The teeth were split, the pulpal tissues removed and fixed in 4% paraformaldehyde in 0.1 M PB for 20 minutes. The pulpal tissue was rinsed in 0.1 M PB and then placed in 30% sucrose in 0.1 M PB overnight at 4°C. The next day the pulp was placed in Neg-50 (Richard-Allan Scientific; Kalamazoo, MI) and stored at −80 °C. Pulpal samples were thawed and embedded in Neg-50, with a normal sample next to a painful sample, and serially sectioned with a cryostat at 30 μms in the longitudinal plane. Sections were placed onto Superfrost Plus slides (Fisher Scientific, Pittsburgh, PA), air dried and then stored at −20° C.

Immunocytochemistry

A single slide was selected from each of the 10 different sample pairs and consisted of sections where the coronal and radicular pulpal regions were fully present. All sample pairs were then double-stained with a pan-specific NaCh antibody (rabbit polyclonal antibody used at 1:100) that identifies a conserved epitope located within the alpha subunit of all NaCh isoforms[13] and antibody against caspr (mouse monoclonal antibody kindly provided by Dr. Peles and used at 1:500) which is highly expressed in the paranodal region of myelinated axons and is used to identify nodes of Ranvier[25], with the use of the indirect immunofluorescence method as previously described.[3,24] Species-specific secondary antibodies (Molecular Probes, Eugene, OR) were used to visualize caspr (Alexa Fluor 488) and NaCh (Alexa Fluor 568) immunofluorescence. The tissue sections that were double-stained were examined with a Nikon PCM-2000 laser scanning confocal microscope. A z-series of optical images (0.8 μm increments) were separately obtained of NaCh and caspr immunofluorescence in nerve fibers within the upper and lower radicular pulp from each sample. All images were obtained with a 40x oil immersion objective lens at a 1024 × 1024 pixel resolution, where each pixel is 0.3 μm in length with an area of 0.09 μm^2, and with identical laser power settings that allowed the identification of multiple pixels with a maximum 255 intensity (8 bit images) in most nodes of Ranvier, while still allowing an obvious gradation of immunofluorescence staining intensities of NaChs present within accumulations.

One section from four normal samples and four painful samples were triple-labeled with antibodies against NaCh, caspr, and myelin basic protein (MBP; Chemicon, Temecula, CA, catalog # MAB386, rat monoclonal used at 1:200 and visualized with Alexa Fluor 633 from Molecular Probes). These triple-labeled specimens were examined with a Nikon C1si confocal microscope and representative images obtained.

Control sections were processed as above except NaCh antibody was mixed with peptide antigen (approximately 30:1 peptide to antibody molar concentration ratio) for a minimum of four hours before application to tissue sections and images were obtained with the same laser gain settings used to visualize NaCh immunofluorescence in the experimental specimens. Other sections were processed identical to experimental sections but with the omission of primary antibodies.

All images were processed for illustration purposes with Adobe Photoshop CS2 (Adobe Systems, San Jose, CA) and CorelDRAW 12 (Corel Corporation, Ottawa, Canada).

Quantitative analysis to determine density and average size of significant NaCh accumulations

Every sixth slice (representing a distance interval of 4.8 μm) within the NaCh only z-series was evaluated with NIH ImageJ software[26] to determine the area occupied by nerves, and the density and average size of significant NaCh accumulations within the nerve area as previously described.[20] Briefly, this involves an outlining of nerve fiber to determine nerve area, a threshold step to remove lower intensity pixels (including those that may represent nonspecific staining) and that limits the NaCh analysis to pixels with a maximum intensity of 255, and then an analyze step that determines the total count and average size of NaCh accumulations with four or more contiguous pixels with maximum intensity within the nerve area. The results from this analysis that was performed on separate images of axon bundles located in the upper and lower radicular region from each sample were then combined to determine density and size of significant accumulations in each individual normal and painful sample.

Analysis to characterize NaCh accumulations at typical and atypical nodal sites

The NaCh-only z-series from select normal and painful samples (see below) was combined with the corresponding caspr-only z-series with ImageJ and each viewed as a maximum intensity collapsed z-projection. A threshold of 255 was applied to the NaCh-only z-series used here so as to limit this analysis to only those pixels with maximum NaCh immunofluorescence intensity, as was done in the density analysis (see above). This thresholded maximum intensity collapsed z-projection was then used to characterize the expression of NaCh accumulations at nodal sites that were classified as either typical or atypical as based on caspr relationships in image stacks obtained from the radicular region of five normal samples and five painful samples. This analysis was limited to those NaCh accumulations that were totally contained within the z-dimension of the stack. The NaCh accumulations that were adjacent to caspr-positive sites were classified as either; (1) typical nodes – NaCh staining fills the gap at the node of Ranvier as identified by the paranodal staining of caspr seen on both sides of the node, (2) split nodes – two distinct NaCh accumulations, separated by a gap in the NaCh staining within the same fiber and with each NaCh accumulation flanked on only one side with caspr staining, or (3) heminodes – caspr staining located on only one side of a contiguous NaCh accumulation or two bands of caspr staining present on both sides of a contiguous NaCh accumulation but where the area of caspr staining was greatly diminished on one side to less than 50% of that seen on the side with more extensive caspr. Those NaCh accumulations that lacked an association with caspr and that had four or more contiguous pixels with a maximum 255 NaCh-immunofluorescence intensity were classified as “naked” accumulations. The analysis of NaCh accumulations at caspr-identified sites was limited to those NaCh accumulations that contained four or more pixels with a maximum 255 NaCh-immunofluorescence intensity. The location of the pixels(s) was confirmed to be at a nodal site by navigation through the various levels of each combined and non-thresholded NaCh and caspr z-stack to verify the presence of other pixels with NaCh immunofluorescence in a pattern consistent with that seen at nodal sites. The heminodes and split-nodes were then considered as a group and classified as atypical nodal sites, whereas the NaCh accumulations that were not associated with caspr were identified as naked accumulations and classified as a separate group. In addition, the width of caspr staining within the paranodal region of every caspr-identified typical and atypical NaCh accumulation present in the area imaged in the upper radicular region of one painful sample was measured to determine axon diameter.

Statistical analysis

Significant differences were determined with the use of the unpaired Student’s *t*-test and standard error of the mean (S.E.M.). The “n” used in these tests equaled the number of image slices evaluated in each sample for the NaCh accumulation size and density analysis, whereas in the evaluation to characterize NaCh accumulations at typical and atypical sites “n” equaled the total number of different samples evaluated in each normal and painful group.

Results

Qualitative description of NaCh localization within normal and painful samples

Evaluation of normal and painful samples showed prominent NaCh expression within large accumulations that were most commonly seen at caspr-identified nodal sites. Many of the painful samples showed extensive carious lesions that involved much of the coronal pulp. The nerve fiber bundles located within the coronal pulp of some of these samples appeared fragmented and associated with this fragmentation was a lack of NaCh expression and a loss of structured caspr staining that is typically restricted to the paranodal region of myelinated normal fibers. In contrast, most of the painful samples showed more intact fibers within radicular areas than seen in the coronal area and so the quantification of NaCh expression was limited to these radicular areas.

Quantitative analysis of NaCh accumulation density and size

A comparison of the NaCh accumulation density (number of accumulations/nerve area in mm^2) seen in the radicular pulp showed a wide range of densities within the individual samples of both the normal and the painful groups (Fig 1). Although the mean density of the painful group was less than the normal group, there was no significance difference in the mean density between these two groups (normal- 971.4 ± 192.9; painful- 560.3 ± 155.9; $p = 0.115$). The total number of accumulations evaluated among all of the normal samples was 610 (range 31–109), while 349 were evaluated in the painful samples (range 1–143). In contrast, a comparison of the mean size of NaCh accumulations showed less variation among the individual samples of the painful group and especially the normal group (Fig 2), and no significance difference between the mean calculated for each group (normal- 10.54 ± 0.75; painful- 10.17 ± 1.04; $p = 0.77$). The limitation of this analysis to only those pixels with a maximum 255 NaCh immunofluorescence intensity and the lack of these pixels in the peptide-blocked control preparations (see below) minimized the chance for the inclusion of non-specific immunofluorescence signal into the results of this analysis.

Quantitative analysis shows increased 'atypical' nodal NaCh accumulations in the painful dental pulp

Examination of the peptide-blocked control preparations showed a lack of NaCh staining within axons and no pixels with a 255 immunofluorescence staining intensity (Fig 3A). In contrast, samples stained with NaCh and caspr antibodies showed a typical pattern of staining relationships in normal samples and variations from this pattern among the different painful samples (Fig 3B–E). In general, NaCh accumulations were most common at caspr-identified typical nodes within the normal samples (Fig 3B), whereas NaCh accumulations were more commonly seen at atypical nodal sites in painful samples with various accumulation densities (Figs 3C–E). Since the NaCh and caspr relationships appeared to vary between normal and painful samples, an analysis was done that characterized NaCh accumulation expression at caspr-identified typical and atypical nodal sites (includes heminodes and split nodes) and within naked accumulations in five normal samples (sample #'s 2, 3, 5, 9 and 10 as identified in Fig 1–Fig 2) and in five painful samples (sample #'s 5–7, 9 and 10 as identified in Fig 1–Fig 2). The results of this analysis are displayed in Table 1 and revealed a significant decrease in the number of NaCh accumulations associated with typical nodes (from 85.8% ±2.4 to 64.1.% ±4.8; $p<0.01$) and an increase in the number of NaCh accumulations associated with atypical nodes (5.7%% ±1.0 to 20.0.% ±5.0; $p<0.05$) and an insignificant increase in the number of naked accumulations (8.6% ±2.4 to 15.9% ±5.2) in the painful dental pulps when compared to those seen in the normal samples (Fig 4). Most accumulations in normal samples were seen at intact nodes of Ranvier, as defined by the paranodal staining of caspr seen on both sides of the node (Fig 5A). Occasionally, NaChs were seen within accumulations that lacked an association with caspr or that showed alterations in caspr relationships such as caspr expression on only one side of the accumulation, but in general these altered relationships were less common in normal samples. In contrast, alterations in NaCh and caspr relationships were more common in painful samples. These alterations included typical nodes with an increased nodal area showing NaCh-immunofluorescence (Fig 5B), and broadened NaCh accumulations that were associated with decreased caspr staining on one or both sides (Figs 5C–F). At times, two closely spaced NaCh accumulations were located within the same fiber and these were separated by single or multiple discrete regions that showed caspr expression (Figs 5G, H). Other altered relationships showed the presence of two closely spaced typical nodes within the same fiber, while other large NaCh accumulations lacked caspr associations altogether (Fig 5I). The results of the size analysis that measured the width of caspr staining within the paranodal region of each caspr-identified NaCh accumulation within the upper radicular region of painful sample #9 found no significant difference between the 1.79 μm average axon diameter for typical nodes (n=24; size range of 1.01–2.95 μms) when compared to the 1.59

μm average axon diameter for atypical nodes (n=15; size range of 0.9–2.82 μm). These results show that the expression of NaCh accumulations at atypical nodal sites within small-diameter axons with a size range consistent with A-delta fibers are commonly seen within painful samples.

Axonal demyelination in painful dental pulps

The increased occurrence of NaCh accumulations at atypical nodal sites seen in the painful dental pulp might reflect a disorganization of normal myelin structure since these forms have been observed during the demyelination-remyelination process.[13] To test for this possibility, the expression of MBP, a protein that exists abundantly in the compact myelin sheath,[18] was examined in normal and painful dental pulps. Most large nerve fibers in normal specimens were associated with bright and continuous MBP immunofluorescence and the NaCh accumulations seen within these fibers were usually seen at typical nodal sites (Fig 6A). In contrast, the MBP staining was less intense, and sometimes focally or even totally absent within nerve fibers in the painful dental pulp samples. The large fibers with these changes in MBP staining at times also showed alterations in NaCh-caspr relationships (Fig 6B). These included the presence of large NaCh accumulations at heminodes, where MBP staining was present along the fiber next to the caspr staining, but where MBP staining was absent in the area of the NaCh accumulation and beyond (Figs 6C–E). Thus, the maintenance of typical nodal NaCh clusters appeared to rely on the existence of normal myelin structures.

Discussion

The results of this study show that the density and size of NaCh accumulations within the radicular regions of painful teeth with large carious lesions varied widely among the different samples when compared to expressions seen in normal teeth. This variation suggests that there is no correlation of overall NaCh density and size of accumulations with the severe and spontaneous pain characteristics that were described by the subjects that provided the painful samples. In contrast, a common finding among the painful samples was the increased occurrence of NaCh accumulations at atypical nodal forms. These atypical nodal forms have been previously observed during the demyelination-remyelination process[5,13] and together with the loss of MBP staining seen in the painful samples, these findings suggest that axonal demyelination within the painful dental pulp is a common event. Given that peripheral nerve demyelination can induce neuropathic pain[19,33] and that spontaneous pain is an important characteristic of neuropathic pain, it is possible that this remodeling of NaChs at these atypical demyelinated nodal sites may contribute to the spontaneous pain paroxysms that were reported by all subjects included in the painful sample group. Therefore the results of our study suggest that one possible contribution of altered NaCh expression to acute pulpal pain mechanisms may relate more to the quality of expression at single sites rather than the overall NaCh axonal content.

Action potential generation and propagation involves the activation of voltage-gated NaChs and changes in expression may contribute to both inflammatory and neuropathic pain mechanisms.[4] The specific NaCh isoforms that are most commonly implicated in this process include the $Na_v1.7$, 1.8 and 1.9 isoforms that are preferentially expressed in the peripheral nervous system and seen in a subset of nociceptors[2,17,31] and $Na_v1.3$ that is reexpressed after injury.[7] Although many animal studies have evaluated changes in NaCh expression after nerve and inflammatory lesions[4], studies that have evaluated expressions within axons located in normal and painful human peripheral tissues are fewer. Most of these human studies have evaluated isoform specific changes in expression after nerve injury and in neuropathic pain conditions,[9–10,23,29,35] whereas studies that have specifically evaluated NaCh expression with the use of a pan-specific antibody that identifies all isoforms is limited to a single study that

evaluated painful neuromas.[16] This lack of knowledge of pan-specific NaCh expression in human inflammatory conditions contrasts sharply with the many studies that have been performed in experimental animals.

Others have used the human dental pulp to evaluate changes in isoform-specific NaCh expression that include the $Na_v1.7$,[24] $Na_v1.8$[27] and $Na_v1.9$[34] isoforms, whereas studies that have evaluated overall NaCh expression with a pan-specific antibody are lacking. In contrast to the highly variable NaCh expression identified in the present study, these isoform-specific studies showed an increased expression of each isoform in the dental pulp from painful teeth. Even though this difference may result from a possible difference in isoform-specific verses pan-specific expression, a more likely explanation involves differences in the extent of the carious lesion and the possible influence of this variable on axon viability and subsequent axonal NaCh expression. Axon degeneration appears to be more extensive within the pulp of teeth with large carious lesions than in teeth with smaller lesions, like the samples evaluated in our $Na_v1.7$ study.[24] So, even though important differences in NaCh expression may result from possible degenerative influences, the qualitative differences in expression seen at isolated sites may be just as important as the total overall and isoform-specific NaCh expression that has typically been the focus of most other studies.

The variable NaCh expression identified within our painful samples is different from the one other human study that evaluated axonal NaCh expression with the use of a pan-specific antibody and that identified an increased expression within painful neuromas when compared to that seen within normal sciatic nerves.[16] Differences between the neuroma study and the present study may relate to basic differences between neuropathic and pulpal pains. Pulpal pain secondary to a carious lesion is typically considered an inflammatory pain condition with important influences provided by bacteria,[8] and the progression of the carious lesion may result in significant pulpal necrosis, associated with an initial remodeling and ultimately a degeneration of nerves within the necrotic zone. These inflammatory and degenerative influences help to differentiate pulpal pain from neuropathic pain and may be related to the decreased NaCh expression seen in some painful samples.

Even though obvious differences exist between pulpal pain and neuropathic pain, nerve involvement represents a feature common to both conditions. One possible consequence of nerve involvement could relate to the presence of spontaneous pain that is considered a hallmark feature of neuropathic pain[30] and that was an inclusion criteria for painful samples included in our study. In this regard, spontaneous pain may represent a neuropathic pain component of pulpal pain. Although the mechanism that produces spontaneous pain is unknown, ectopic discharge at isolated sites with high NaCh density, like the ones commonly seen in the painful samples, is one possibility.[12] These large NaCh accumulations were common in small-diameter myelinated fibers, where their activation could contribute to the sharp, shooting characteristics of spontaneous pulpal pain that originates from A-delta fibers.[1] Other evidence that supports a possible neuropathic pain component associated with toothache is the common occurrence of atypical nodal forms seen in our painful samples that are also encountered at the site of injury produced by chromic suture in the chronic constriction injury model for neuropathic pain.[20] The chromic suture injury produces a robust inflammatory cell infiltrate, somewhat like that seen within the dental pulp. The frequent occurrence of atypical nodal forms and of inflammatory cells in both suggests important peripheral neuro-glial-immune interactions that may be involved in the production of specific pain characteristics such as spontaneous pain that are common to both pulpal pain and neuroinflammatory neuropathic pain conditions.

Atypical nodal forms were common in our painful samples and these forms are seen during the demyelination-remyelinating process.[5,13] Additionally, the loss of MBP staining observed

in our painful samples suggests that demyelination influences are prominent within the painful dental pulp. Others have shown a similar loss of myelin staining within demyelinating lesions with antibodies against MBP,[32] myelin oligodendrocyte glycoprotein[22] and myelin-associated glycoprotein.[5] Furthermore, the identification of single fibers with multiple nodes that are separated by short distances is the same as those seen within remyelinating lesions of patients with multiple sclerosis[22] and their presence suggests previous demyelinating influences. Previous studies have shown that the disruption of myelin results in profound changes in NaCh expression in axons[13–16,20] similar to the changes identified in the present study. The remodeling of NaChs within demyelinating fibers described here follows our previous description of the same process in a study that evaluated human $Na_v1.7$ pulpal expression and these findings suggest demyelination as a basic pulpal pain mechanism.

Even though our study was limited to NaCh expression within nodal-like accumulations, expressions in unmyelinated fibers are also important since pulpal pain mechanisms involve the activation of both myelinated and unmyelinated axons.[6] Future studies are needed to further evaluate the expression of overall NaCh and isoform specific NaCh expressions within myelinated and unmyelinated fibers and to correlate such changes with the presence or absence of specific pain characteristics such as those toothaches characterized by only dull toothache pain as compared to those with sharp, shooting spontaneous pain. These future evaluations may provide important findings that may correlate specific NaCh changes with certain pain characteristics.

One of the challenges encountered when studying pain mechanisms from dental pulp samples is the identification of those critical events that are most closely linked with the transition from a hyperalgesic state to an acute and severe pain state. Many individuals who opt for tooth extraction due to pain have experienced a gradual escalation in pain responses following sensory stimulation, but tolerate these hyperalgesic responses and only seek care when the pain worsens. One pain characteristic that often times prompt immediate care is the presence of sharp, shooting spontaneous pain. The study of such samples may provide important information regarding changes that may correlate with this important transition from a hyperalgesic to an acute and severe pain condition. While the findings of our study describe a wide range in the density and size of NaCh accumulations located within the radicular pulp of painful samples, we found that atypical nodal forms are significantly more common in these same samples. Altogether, these findings suggest that a contribution of altered NaCh expression to pulpal pain mechanisms may relate to the quality of such changes at individual sites rather than to the overall changes in expression and point to the importance of studies that evaluate specialized subcellular domains within individual fibers.

Acknowledgements

This work was supported by NIH Grant DE015576 from the National Institute of Dental and Craniofacial Research. We thank Dr. E. Peles for his generosity in providing the anti-caspr antibody.

References

1. Ahlquist ML, Franzen OG. Encoding of the subjective intensity of sharp dental pain. Endod Dent Traumatol 1994;10:153–166. [PubMed: 7995246]
2. Akopian AN, Sivilotti L, Wood JN. A tetrodotoxin-resistant voltage-gated sodium channel expressed by sensory neurons. Nature 1996;379:257–262. [PubMed: 8538791]
3. Alvarado LT, Perry GM, Hargreaves KM, Henry MA. TRPM8 Axonal expression is decreased in painful human teeth with irreversible pulpitis and cold hyperalgesia. J Endod 2007;33:1167–1171. [PubMed: 17889683]

4. Amir R, Argoff CE, Bennett GJ, Cummins TR, Durieux ME, Gerner P, Gold MS, Porreca F, Strichartz GR. The role of sodium channels in chronic inflammatory and neuropathic pain. J Pain 2006;7:S1–S29. [PubMed: 16632328]
5. Arroyo EJ, Sirkowski EE, Chitale R, Scherer SS. Acute demyelination disrupts the molecular organization of peripheral nervous system nodes. J Comp Neurol 2004;479:424–434. [PubMed: 15514980]
6. Bender IB. Pulpal pain diagnosis--a review. J Endod 2000;26:175–179. [PubMed: 11199715]
7. Black JA, Cummins TR, Plumpton C, Chen YH, Hormuzdiar W, Clare JJ, Waxman SG. Upregulation of a silent sodium channel after peripheral, but not central, nerve injury in DRG neurons. J Neurophysiol 1999;82:2776–2785. [PubMed: 10561444]
8. Byers MR, Narhi MV. Dental injury models: experimental tools for understanding neuroinflammatory interactions and polymodal nociceptor functions. Crit Rev Oral Biol Med 1999;10:4–39. [PubMed: 10759425]
9. Coward K, Aitken A, Powell A, Plumpton C, Birch R, Tate S, Bountra C, Anand P. Plasticity of TTX-sensitive sodium channels PN1 and brain III in injured human nerves. Neuroreport 2001;12:495–500. [PubMed: 11234752]
10. Coward K, Plumpton C, Facer P, Birch R, Carlstedt T, Tate S, Bountra C, Anand P. Immunolocalization of SNS/PN3 and NaN/SNS2 sodium channels in human pain states. Pain 2000;85:41–50. [PubMed: 10692601]
11. Cummins TR, Sheets PL, Waxman SG. The roles of sodium channels in nociception: Implications for mechanisms of pain. Pain 2007;131:243–257. [PubMed: 17766042]
12. Devor M. Sodium channels and mechanisms of neuropathic pain. J Pain 2006;7:S3–S12. [PubMed: 16426998]
13. Dugandzija-Novakovic S, Koszowski AG, Levinson SR, Shrager P. Clustering of Na+ channels and node of Ranvier formation in remyelinating axons. Journal of Neuroscience 1995;15:492–503. [PubMed: 7823157]
14. England JD, Gamboni F, Levinson SR. Increased numbers of sodium channels form along demyelinated axons. Brain Res 1991;548:334–337. [PubMed: 1651145]
15. England JD, Gamboni F, Levinson SR, Finger TE. Changed distribution of sodium channels along demyelinated axons. Proc Natl Acad Sci U S A 1990;87:6777–6780. [PubMed: 2168559]
16. England JD, Happel LT, Kline DG, Gamboni F, Thouron CL, Liu ZP, Levinson SR. Sodium channel accumulation in humans with painful neuromas. Neurology 1996;47:272–276. [PubMed: 8710095]
17. Fang X, Djouhri L, Black JA, Dib-Hajj SD, Waxman SG, Lawson SN. The presence and role of the tetrodotoxin-resistant sodium channel Na(v)1.9 (NaN) in nociceptive primary afferent neurons. J Neurosci 2002;22:7425–7433. [PubMed: 12196564]
18. Garbay B, Heape AM, Sargueil F, Cassagne C. Myelin synthesis in the peripheral nervous system. Prog Neurobiol 2000;61:267–304. [PubMed: 10727776]
19. Gillespie CS, Sherman DL, Fleetwood-Walker SM, Cottrell DF, Tait S, Garry EM, Wallace VC, Ure J, Griffiths IR, Smith A, Brophy PJ. Peripheral demyelination and neuropathic pain behavior in periaxin-deficient mice. Neuron 2000;26:523–531. [PubMed: 10839370]
20. Henry MA, Freking AR, Johnson LR, Levinson SR. Increased sodium channel immunofluorescence at myelinated and demyelinated sites following an inflammatory and partial axotomy lesion of the rat infraorbital nerve. Pain 2006;124:222–233. [PubMed: 16828970]
21. Hille, B. Ion Channels of Excitable Membranes. Sunderland Sinauer: 2001.
22. Howell OW, Palser A, Polito A, Melrose S, Zonta B, Scheiermann C, Vora AJ, Brophy PJ, Reynolds R. Disruption of neurofascin localization reveals early changes preceding demyelination and remyelination in multiple sclerosis. Brain 2006;129:3173–3185. [PubMed: 17041241]
23. Kretschmer T, Happel LT, England JD, Nguyen DH, Tiel RL, Beuerman RW, Kline DG. Accumulation of PN1 and PN3 sodium channels in painful human neuroma-evidence from immunocytochemistry. Acta Neurochir (Wien) 2002;144:803–810. [PubMed: 12181690]discussion 810
24. Luo S, Perry GM, Levinson SR, Henry MA. Nav1.7 expression is increased in painful human dental pulp. Mol Pain 2008;4:16. [PubMed: 18426592]

25. Poliak S, Gollan L, Martinez R, Custer A, Einheber S, Salzer JL, Trimmer JS, Shrager P, Peles E. Caspr2, a new member of the neurexin superfamily, is localized at the juxtaparanodes of myelinated axons and associates with K+ channels. Neuron 1999;24:1037–1047. [PubMed: 10624965]

26. Rasband, WS. ImageJ. 1997–2007. http://rsb.info.nih.gov/ij/

27. Renton T, Yiangou Y, Plumpton C, Tate S, Bountra C, Anand P. Sodium channel Nav1.8 immunoreactivity in painful human dental pulp. BMC Oral Health 2005;5:5. [PubMed: 16001984]

28. Rzasa R, Henry M, Johnson L, Levinson S. Quantitative analysis of sodium channel expression in normal and painful human teeth. J Pain. 2006

29. Shembalkar PK, Till S, Boettger MK, Terenghi G, Tate S, Bountra C, Anand P. Increased sodium channel SNS/PN3 immunoreactivity in a causalgic finger. Eur J Pain 2001;5:319–323. [PubMed: 11558987]

30. Thomas, P. Peripheral Neuropathy. Vol. Vol 2. Philadelphia: WB Saunders; 1984. Clinical features and differential diagnosis of peripheral neuropathy; p. 1169-1190.

31. Toledo-Aral JJ, Moss BL, He ZJ, Koszowski AG, Whisenand T, Levinson SR, Wolf JJ, Silos-Santiago I, Halegoua S, Mandel G. Identification of PN1, a predominant voltage-dependent sodium channel expressed principally in peripheral neurons. Proc Natl Acad Sci U S A 1997;94:1527–1532. [PubMed: 9037087]

32. Trapp BD, Peterson J, Ransohoff RM, Rudick R, Mork S, Bo L. Axonal transection in the lesions of multiple sclerosis. N Engl J Med 1998;338:278–285. [PubMed: 9445407]

33. Wallace VC, Cottrell DF, Brophy PJ, Fleetwood-Walker SM. Focal lysolecithin-induced demyelination of peripheral afferents results in neuropathic pain behavior that is attenuated by cannabinoids. J Neurosci 2003;23:3221–3233. [PubMed: 12716929]

34. Wells JE, Bingham V, Rowland KC, Hatton J. Expression of Nav1.9 channels in human dental pulp and trigeminal ganglion. J Endod 2007;33:1172–1176. [PubMed: 17889684]

35. Yiangou Y, Birch R, Sangameswaran L, Eglen R, Anand P. SNS/PN3 and SNS2/NaN sodium channel-like immunoreactivity in human adult and neonate injured sensory nerves. FEBS Lett 2000;467:249–252. [PubMed: 10675548]

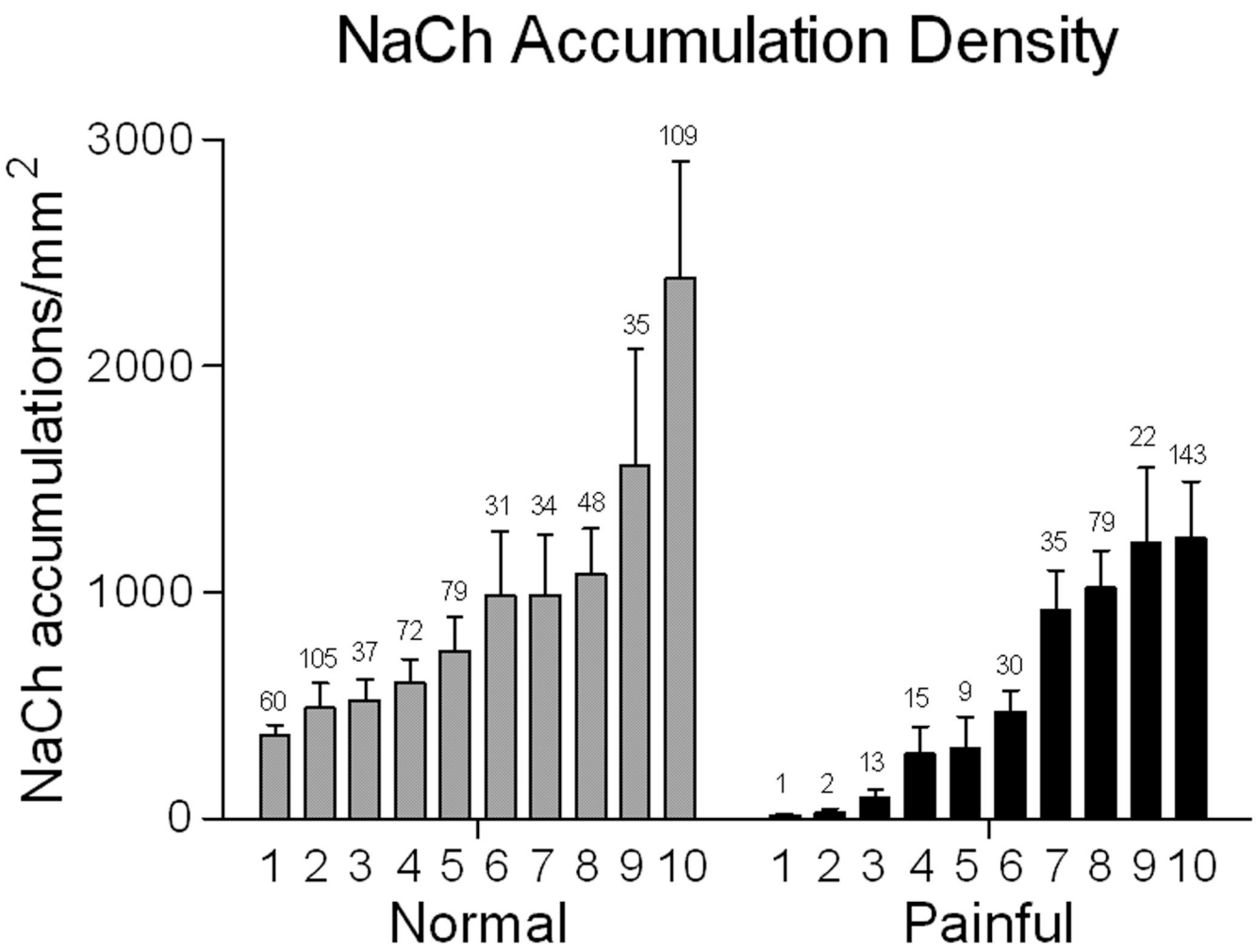

Figure 1.

The density of NaCh accumulations (number of accumulations/mm^2 nerve area) seen within the radicular region of both normal (*grey bars*) and painful (*black bars*) samples varies widely among the different individual samples within each group and statistical analysis showed no significant difference in density between the normal and painful groups. The number above each bar represents the total number of accumulations identified within the upper and lower radicular areas in one section from each of the ten normal and ten painful samples evaluated in the study.

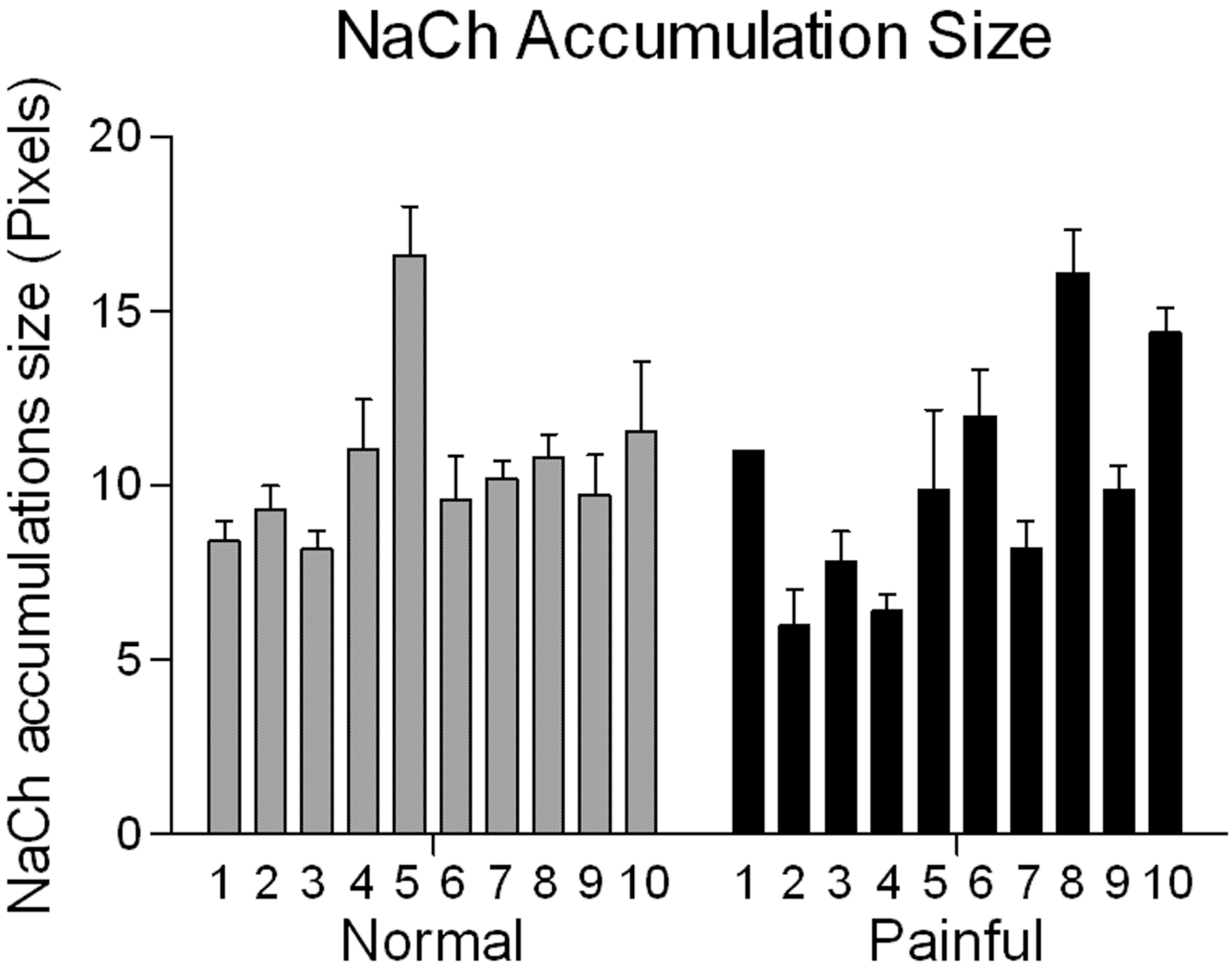

Figure 2.
The average size (in number of pixels) of NaCh accumulations seen within the radicular region of both normal (*grey bars*) and painful (*black bars*) samples varies among the different individual samples within each group and statistical analysis showed no significant difference in accumulation size between the normal and painful groups.

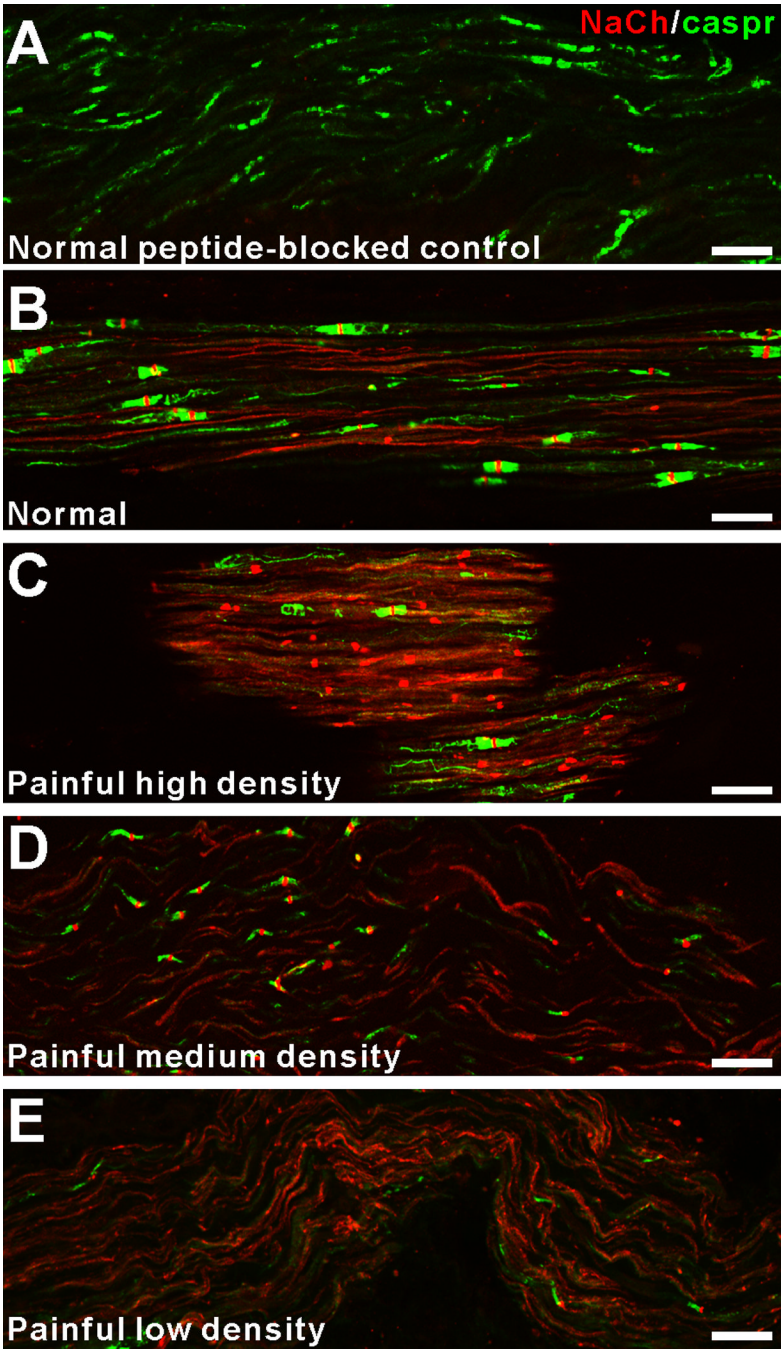

Figure 3.

The expression of NaCh accumulations is variable in painful samples. Confocal micrographs (collapsed z-projection images of five separate image slices separated by 1 μm increments) demonstrate NaCh (red) and caspr (green) staining relationships in a normal peptide-blocked control sample (A), a normal sample (B; from normal sample #5) and in three different painful samples (C–E). The peptide-blocked control sample shows a lack of NaCh staining within caspr-identified axons (A). The NaCh accumulations within the normal sample are most common at caspr-identified typical nodal sites (B), while NaCh accumulations at atypical nodal sites are common in painful samples with high (C; from painful sample #8), medium (D; from painful sample #4) and low (E; from painful sample #3) densities. Scale bars = 20 μm.

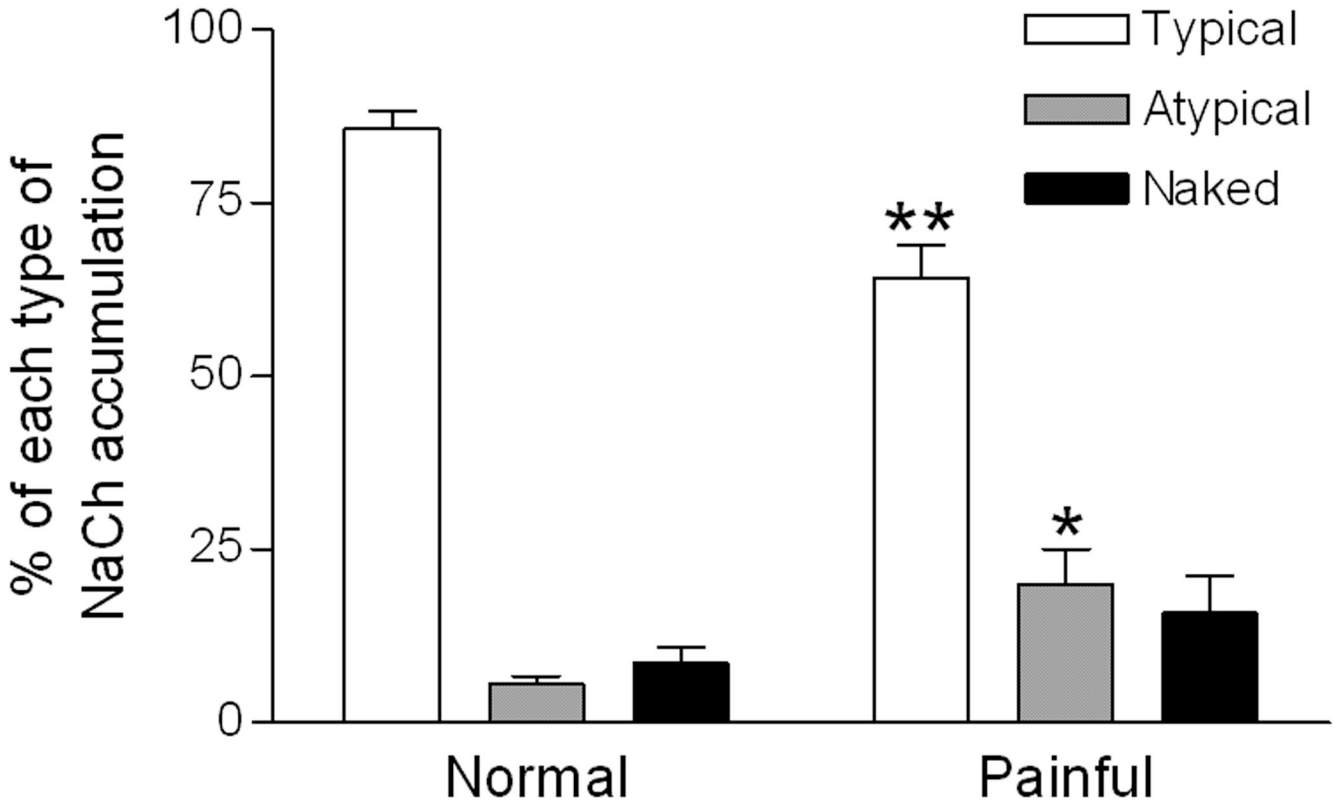

Figure 4.

Characteristics of NaCh accumulations at caspr-associated nodal sites change in painful pulp. Results show a significant increase in the proportion of NaCh accumulations at atypical nodal sites (heminodes and split nodes) and a significant decrease at typical nodes in the painful dental pulp when compared to the proportions seen in normal samples. Although naked accumulations were more common in painful samples than in normal samples, the difference was not significant. * = $p < 0.05$; ** = $p < 0.01$.

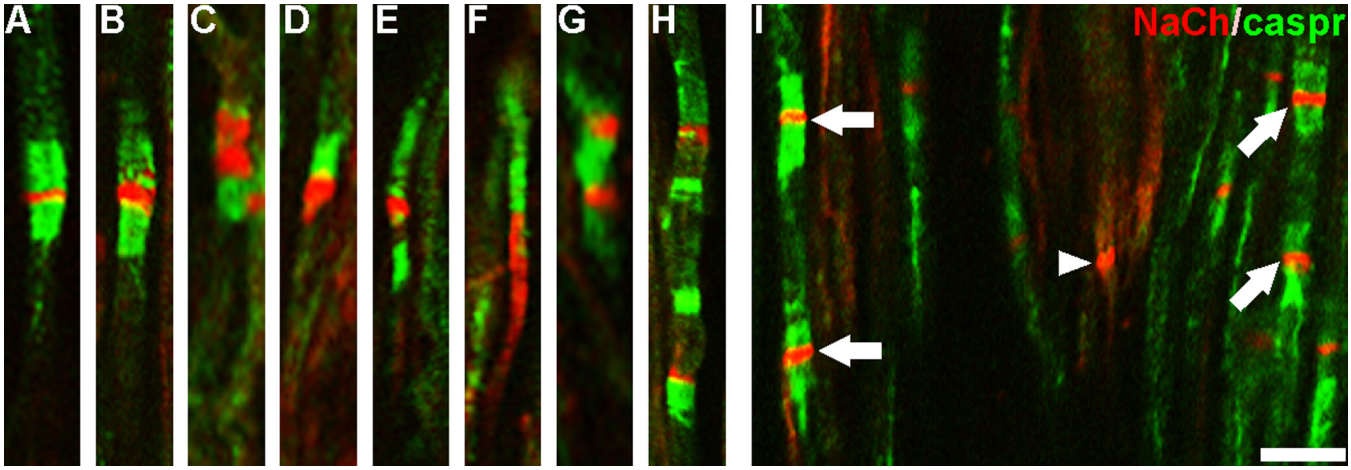

Figure 5.

NaCh and caspr relationships at nodal sites are altered in painful dental pulp. Confocal micrographs of individual image slices show NaCh (red) and caspr (green) staining relationships in a normal (A) and painful (B–I) samples. The NaChs are located in the narrow nodal gap and are flanked by dense paranodal caspr staining in a typical node from a normal sample (A), whereas deviations from this relationship are seen in NaCh accumulations identified in painful samples. These deviations include enlarged NaCh accumulations that show a decreased intensity or even an elimination of caspr staining on one side of the NaCh accumulation (B–F), while other single fibers show multiple NaCh accumulations (arrows) separated by short distances that show atypical (G–H) and typical (I) caspr relationships. Some NaCh accumulations lacked associations with caspr (arrowhead). Scale bar = 10 μm.

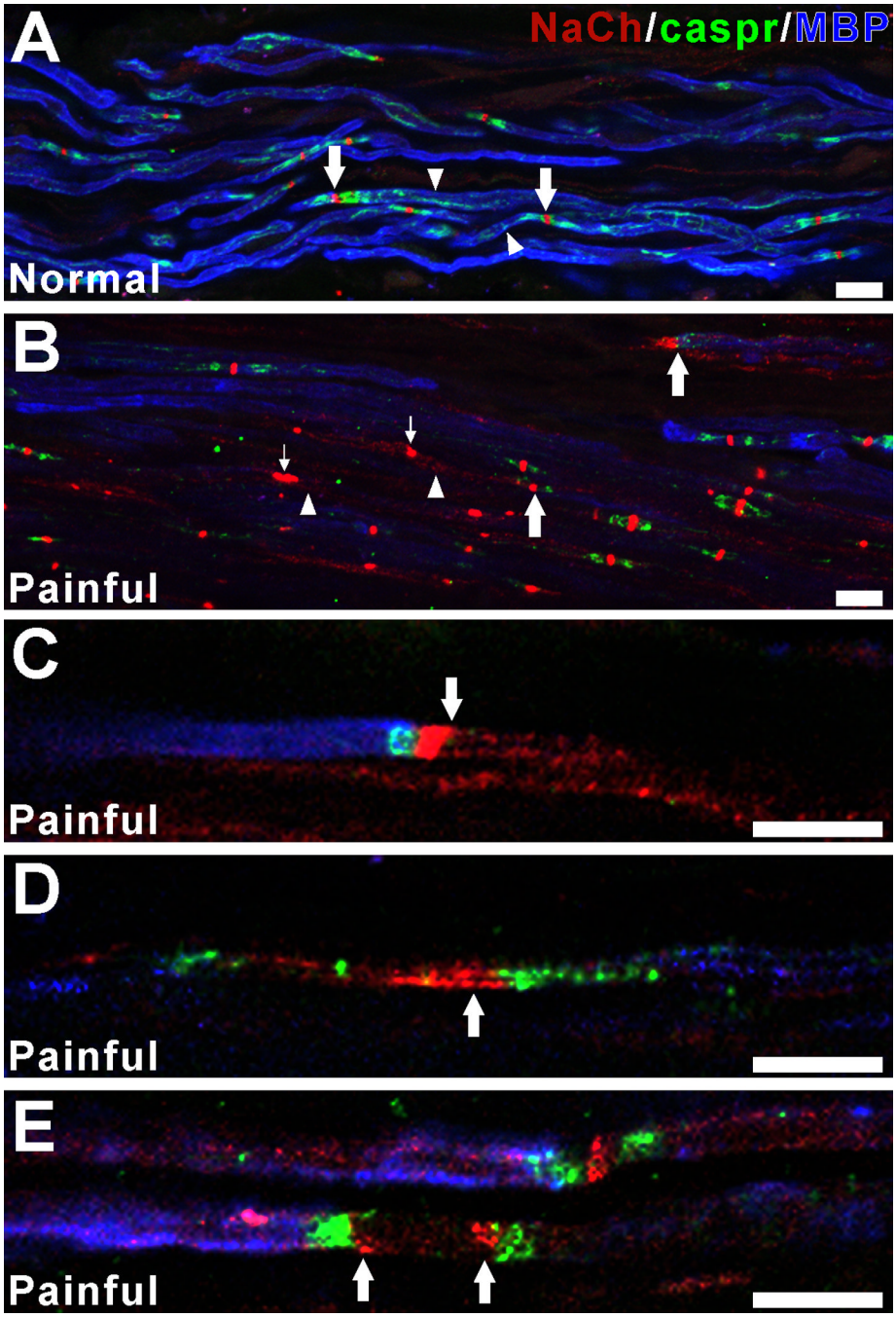

Figure 6.

Painful samples show NaCh expression in fibers with decreased staining for myelin basic protein (MBP). Confocal micrographs of collapsed z-projection images (A, B; five separate image slices separated by 1 μm increments) and single image slices (C–E) show NaCh (red), caspr (green) and MBP (blue) staining relationships within a normal sample (A) and variations from this pattern in painful samples (B–E). Myelinated fibers within the normal dental pulp (A) show prominent surface staining for MBP (arrowheads) and NaCh accumulations at caspr-identified typical nodal sites (arrows). In contrast, the painful sample (B) shows generalized and focal areas of decreased MBP staining (arrowheads) and prominent NaCh accumulations at sites that lack caspr (small arrows) and at other sites that show alterations in caspr

relationships (large arrows). The remodeling of NaChs at caspr-identified atypical nodal sites within single fibers that show decreased staining for MBP is shown in C–E. This remodeling includes prominent NaCh expression within axon segments that are flanked by caspr and that lack MBP staining (C–E; arrows). These findings are consistent with the remodeling of NaChs at demyelinated sites within the painful dental pulp. Scale bars = 10μm.

Table 1

Characterization of NaCh Accumulations at Caspr-Identified Sites and in Naked Accumulations

Sample Type	Sample Number	Number of NaCh Accumulations	Typical Nodal Accumulations	Atypical Nodal Accumulations	Naked Accumulations
Normal	2	106	91.5 % (97)	6.6% (7)	1.9% (2)
	3	50	84.0 % (42)	8.0% (4)	8.0% (4)
	5	86	79.1% (68)	7.0% (6)	13.9% (12)
	9	35	82.9 % (29)	2.9% (1)	14.2 % (5)
	10	104	91.3 % (95)	3.9% (4)	4.8% (5)
	Total	381	85.8% ±2.4	5.7%±1.0	8.5%±2.4
Painful	5	46	54.3% (25)	17.4% (8)	28.3% (13)
	6	16	75.0 % (12)	25.0% (4)	0% (0)
	7	74	75.7% (56)	6.8% (5)	17.5% (13)
	9	44	54.5% (24)	36.4% (16)	9.1% (4)
	10	133	60.9% (81)	14.3% (19)	24.8% (33)
	Total	313	64.1% ±4.8	20.0%±5.0	15.9%±5.2